Applications of Magnetic Resonance Imaging to Ion-Exchange Resins

ANTON S. WALLNER[1,*] and WILLIAM M. RITCHEY[2]

[1]Department of Chemistry, Missouri Western State College, St. Joseph, Missouri 64507; [2]Department of Chemistry, Case Western Reserve University, Cleveland, Ohio 44106

SYNOPSIS

Magnetic resonance imaging (MRI) was used to determine swollen resin morphology in cation-exchange beads. The study of the nonuniformity of the swelling of cation-exchange beads [sulfonated styrene–divinylbenzene (SDVB) copolymers] is of interest because the exchange kinetics and other properties are expected to be strongly influenced by the swelling. MRI can replace current invasive and destructive methods for studying the morphology of these resins. Several types of ion-exchange resins were examined including beads which exhibit homogeneous swelling, heterogeneous swelling, and partially sulfonated beads. The variation in intensity observed is due to a variation in crosslink density, degree of sulfonation, composition, sulfone bridging, or a combination of these variables. Due to their small size, the beads were also imaged using a small coil insert. Results are compared to commercially available insert images in terms of signal-to-noise and experiment time. © 1995 John Wiley & Sons, Inc.

INTRODUCTION

Synthetic ion-exchangers have been in use since the 1930s. Today, the most popular exchange materials are based on crosslinked polystyrene–divinylbenzene.[1] Other ion-exchange resins include poly(methyl methacrylate)–polystyrene,[2-4] poly(butyl acrylate)–polystyrene,[5] and latex–polystyrene[6,7] with varying morphologies. The most common cation exchangers have either the sulfonic group ($-SO_3H$) or the carboxylic group ($-COOH$) as the active site.

The sulfonated derivative of linear polystyrene could be used as a cation-exchange resin, but it does not possess good properties for an ion-exchange resin. By adding about 8% divinylbenzene as a crosslinking agent, the polymer becomes mechanically stronger and less porous, becomes less soluble in water, swells less in water, and undergoes a change in the equilibrium constant for the exchange reaction to allow for good ion-exchange properties.[8] The structure of sulfonated polystyrene–divinylbenzene crosslinked ion-exchange resin (SDVB) is shown in Figure 1. The typical sulfonated SDVB resin has a high molecular weight and is insoluble in, but permeable to, water. The sulfonated SDVB resin swells when wet, but the amount of swelling is controlled by the crosslinking: The greater the crosslinking, the less the swelling.[1]

Ion-exchange resins can have various morphologies depending on preparation method, type of polymerization process,[3] type and amount of crosslinking agent added,[8] monomer concentration,[9] type of initiator used,[4] polymer molecular weight,[10] and difference in hydrophilicity of the two polymers.[2,5,11,12] By varying some or many of these parameters, numerous morphologies, each having certain kinetics and exchange properties, have been polymerized. These include confettilike, raspberrylike, void-containing, core–shell, half-moon, sandwichlike, and inverted core–shell.[2-4,6,7]

The control of morphology, from a scientific standpoint, is accomplished by a combination of thermodynamic and kinetic forces. Berg et al. reported the thermodynamic considerations for ion-exchange resins such that the structure with minimal interfacial tensions constituted the thermodynamically favored arrangement.[13] The kinetic forces

* To whom correspondence should be addressed.

Journal of Applied Polymer Science, Vol. 57, 1–6 (1995)
 CCC 0021-8995/95/010001-06

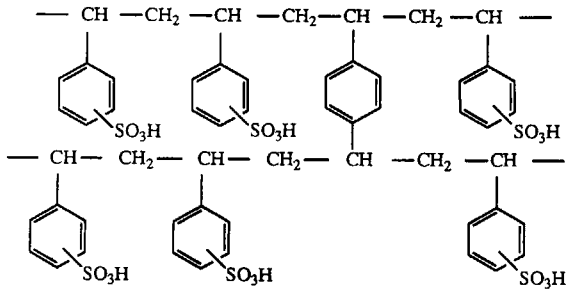

Figure 1 Structure of crosslinked sulfonated polystyrene–divinylbenzene ion-exchange resin.

are essentially the degree of mobility of the polymeric phase.[7] This determines the kinetic control of the battle between the low-energy state and some other structure. The result is a complex combination of thermodynamic and kinetic forces that control the resin morphology.

Analysis of ion-exchange beads has been, until this point, done invasively. The beads have been cut and studied by microscopy[9] and other spectroscopic methods including ESR, SEM, and TEM.[2–4,14,15] Another group of methods has involved staining the ion-exchange resin with RuO_4 or OsO_4 to highlight the double bonds in the resin, sectioning the bead with an ultramicrotome, and scanning these thin sections with transmission electron microscopy.[5,16,17] A final method employs placing the dried beads in an ion sputter and coating with a layer of gold about 500 nm thick. Scanning electron micrographs of these modified beads were obtained and the three-dimensional shapes observed.[4] All these methods yield little information about the bead in the swollen state.

This study shows the first application of MRI to visualize swollen ion-exchange beads prepared by suspension polymerization and their morphology. MRI is an ideal, noninvasive technique to view variations in the degree of swelling these beads exhibit when placed in an appropriate solvent. The nonuniformity of swelling of sulfonated styrene–divinylbenzene beads is an important area of study because the exchange kinetics and other chromatographic properties of the beads are expected to be influenced by the degree of swelling.[18] Several different ion-exchange beads were examined using both a conventional insert and a small coil insert. Results of each are reported.

EXPERIMENTAL

Several types of ion-exchange resins (sulfonated SDVB beads) were obtained from The Dow Chemical Co., Midland, MI. These included ion-exchange beads that exhibit homogeneous swelling, beads that show heterogeneous swelling, and partially sulfonated SDVB beads. These ion-exchange cation resins were prepared by sulfonating SDVB copolymer precursors. The precursors were made via suspension polymerization.[19] The beads were swollen with distilled water before study by MRI. The swollen resins varied in diameter from 0.5 to 2.0 mm.

Various mounting techniques were employed for placing the beads in the NMR tube. First, multiple beads that exhibit homogeneous swelling were placed in a 5 mm-o.d. precision NMR tube (Norell, Inc. Mays Landing, NJ) surrounded by distilled water. Several single-bead mounting methods were attempted. The method of choice positioned one swollen ion-exchange resin in a capillary tube (or on top if the bead was large enough in diameter). The capillary tube was placed in a 5 mm-o.d. NMR tube and positioned in the center of the rf coil by placing a glass rod in the bottom of the NMR tube and a piece of glass around the capillary tube. This arrangement positioned the bead in the center of the rf coil and prevented movement in any direction.

All MRI experiments were performed on a Bruker MSL-400 with microimaging accessory. The nucleus observed was proton at a frequency of 400.130 MHz. A conventional spin-echo sequence was used which employed a soft (selective) 90° pulse and a hard (nonselective) 180° pulse. A 10 mm rf coil was placed in the probe to accommodate the 5 mm NMR tube. One size smaller tube is used to lessen the effects of rf inhomogeneities within the coil by reducing sample cross section.[20] There were 128 phase-encode steps and 128 values for frequency encoding, giving a pixel dimension of 128 × 128. The slice thickness was 0.5 mm. Gradient strengths of 30 G/cm in the x-direction, 26 G/cm in the y-direction, and 4.7 G/cm in the z-direction were employed. The field of view (FOV) was 4.2 mm, giving an in-plane resolution of 33 μm/pixel. The echo time of the spin–echo sequence was 9.66 ms and the repetition time was varied between 0.250 and 1.0 s.

A prototype of the Magnifier developed by Dave Cory at Bruker Instruments, Billerica, MA, was used with a spin–echo sequence to compare results with the conventional 10 mm insert. The Magnifier has a coil with an i.d. of 2.5 mm. Parameters of the experiment were 128 phase- and frequency-encode values, giving a pixel dimension of 128 × 128. The slice thickness was 0.5 mm. Gradient strengths of 30 G/cm in the x-direction, 24.7 G/cm in the y-direction, and 4.7 G/cm in the z-direction were used. The FOV was 2.0 mm, giving an in-plane resolution

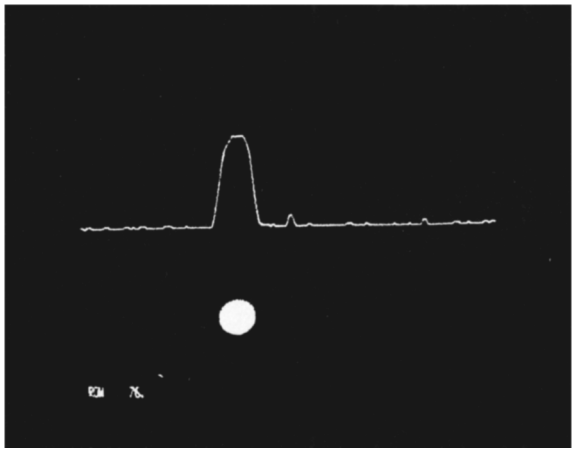

Figure 2 Single, water-swollen sulfonated SDVB bead mounted in a capillary tube.

of 16 μm/pixel. The echo time was 9.66 ms and the repetition time was either 0.250 or 1.0 s. All final images of the resins were postprocessed on an Everex 386 computer using Ansel software to convert the images to laser quality.

RESULTS AND DISCUSSION

Multiple sulfonated SDVB ion-exchange beads were imaged first in an effort to choose the best mounting method for visualization of solvent distribution throughout the beads. The ion-exchange resins were placed in distilled water, allowed to swell, and imaged at room temperature in a 5 mm NMR tube. Several things were observed in these images including no apparent uniformity of bead size or consistent swelling with solvent. The beads vary in size, shape, and degree of swelling. Ion-exchange beads prepared by suspension and/or emulsion polymerization have been reported to be spherical due to surface tension forces which exist during the polymerization process.[2,5,21] Since the image obtained using the multiple-bead method does not show the beads to be spherical with homogeneous solvent distribution, it is not an appropriate mounting technique and was not pursued further.

The final mounting method attempted gave the best results in terms of image quality and accurate representation of the material. This construction employed a glass rod at the bottom of the NMR tube to provide the correct positioning of the sample along the vertical z-axis. The swollen bead with no external solvent was placed in a capillary tube that was heated and drawn out to a narrow point. Figure 2 shows an image of a successfully mounted bead using this glass rod/capillary combination. The intensity of the image is homogeneous throughout the bead. This homogeneous intensity represents homogeneous solvent distribution in the ion-exchange bead. The row profile taken through row 76 (the center of the bead) confirms the visually observed homogeneity with a constant intensity profile. The shape of the bead is circular in the image also. This mounting technique was used in all the subsequent single-bead imaging experiments.

Since the swollen resin was not surrounded by solvent in the single-bead mounting technique, solvent evaporation from the bead became a possible cause of intensity variation in the images. A set of consecutive experiments were run on a homogeneous bead, and the intensity was measured as a function of time. The bead was imaged for six consecutive 2.2 h experiments for a total time of 13.2 h. Intensity measurements were taken from the row profile of the bead at the same position.

Table I is a collection of intensity values from each of the six experiments. The values show a consistent intensity for each of the six experiments. Over the 13.2 h, the intensity varied by only 1.8%. Since all experimental parameters were kept constant, only proton density contributes to intensity in this collection of experiments. Therefore, solvent concentration is proportional to intensity. By only varying 1.8% in intensity over the 13.2 h, the beads do not lose an appreciable amount of solvent due to evaporation over the experiment time of 2.2 h. Therefore, the intensity that is observed is due to solvent distribution and is not an evaporation artifact.

Another collection of ion-exchange beads were examined that demonstrated inhomogeneous solvent distribution when swollen with water. Beads prepared by emulsion and suspension polymerization show similar nonuniformities in solvent uptake.[2,5,21] This nonuniformity in solvent uptake could be due to a variation in crosslink density, degree of sulfo-

Table I Intensity vs. Time for Sulfonated SDVB Bead

Time (h)	Intensity
2.2	10.834
4.4	10.928
6.6	10.925
8.8	10.756
11.0	10.766
13.2	10.735
	Average 10.824 ± 0.086

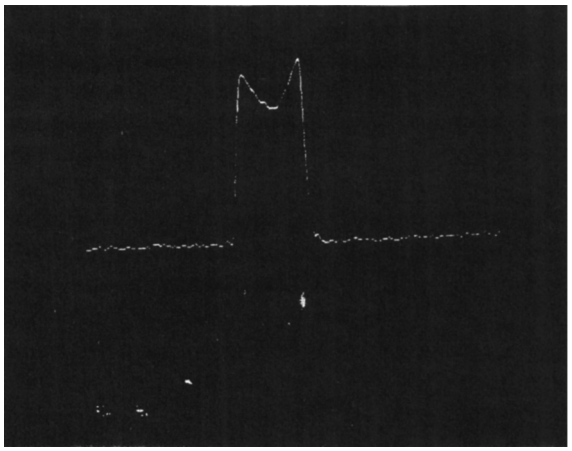

Figure 3 Sulfonated SDVB resin showing inhomogeneous swelling with water. TR = 250 ms.

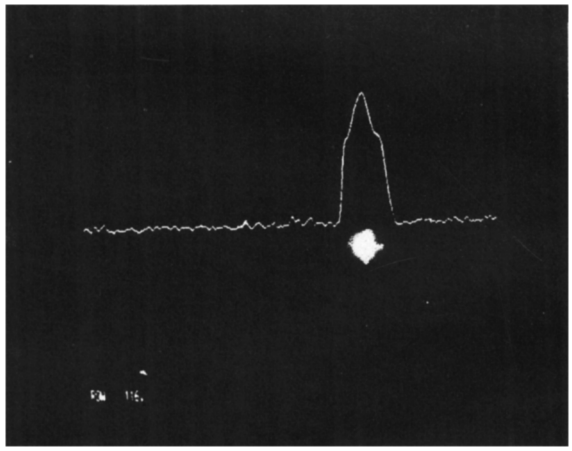

Figure 4 Sulfonated SDVB resin showing inhomogeneous swelling with water. TR = 1 s.

nation, composition, sulfone bridging, or some combination of these variables depending on the details of the synthesis.[18] Figure 3 shows an image of an ion-exchange bead with inhomogeneous solvent distribution. This is seen both visually and with the row profile. The two regions of solvent are expected to have different T_1 values based on how tightly bound the solvent is in each region.[22,23] This prediction was found to hold in this case. The two regions have vastly different T_1 values. The interior region has a T_1 value of 180 ms, whereas the exterior region has a T_1 of 30 ms.[24] This difference is probably due to how tightly bound the solvent is in these two regions and how much solvent is "bulklike" in the regions. Since the experiment in Figure 3 used a repetition time, TR, of 250 ms, the signal arising from the solvent in the interior region is effectively saturated due to the fact that the repetition time is less than $5T_1$. This effect is observed in Figure 3 where intensity is seen only in the exterior ring. The value of TR was chosen without prior knowledge of the T_1 value.

By increasing the repetition time to 1 s, the experiment gave an image that represents the solvent concentration in the swollen resin without loss of intensity due to saturation. Figure 4 shows the image of an ion-exchange resin from the same preparative scheme as in Figure 3, but with an increase in TR to 1 s. The intensity in the interior region is higher than the exterior region, showing a larger concentration of solvent in the interior region. This bead has a more hydrophilic interior and a more hydrophobic exterior based on the solvent swelling observed in Figure 4. This variation in intensity is also seen in the row profile. The shoulder on the row profile represents the intensity in the exterior hydrophobic region, and the peak represents the intensity in the interior, hydrophilic region. By measuring the intensity values in each region from the row profile, a relative quantitative value for the distribution of solvent in the two regions can be obtained. These values from four experiments are listed in Table II. This data shows that in this ion-exchange bead that exhibits inhomogeneous solvent swelling the interior region contains approximately 1.6 times more water due to swelling than does the exterior region. Therefore, the interior region is more hydrophilic than is the exterior region.

Ion-exchange resins can also be prepared by sulfonating only a particular region. When these beads are swollen with water, the sulfonated, hydrophilic

Table II Intensity Values for Sulfonated SDVB Beads

Exterior (Intensity)	Interior (Intensity)	Ratio
TR = 250 ms		
22.960	16.537	0.720
22.798	16.328	0.716
22.485	16.281	0.724
22.116	16.212	0.733
		0.727 ± 0.008
TR = 1 s		
10.374	15.881	1.531
9.791	15.970	1.631
9.931	15.414	1.552
9.184	15.090	1.643
		1.589 ± 0.056

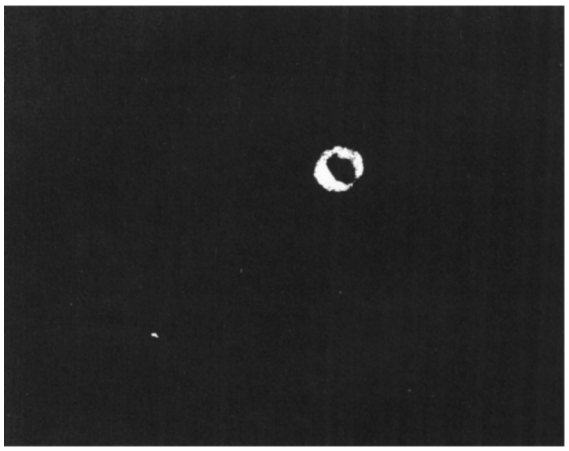

Figure 5 Partially sulfonated SDVB resin swollen with water. TR = 250 ms.

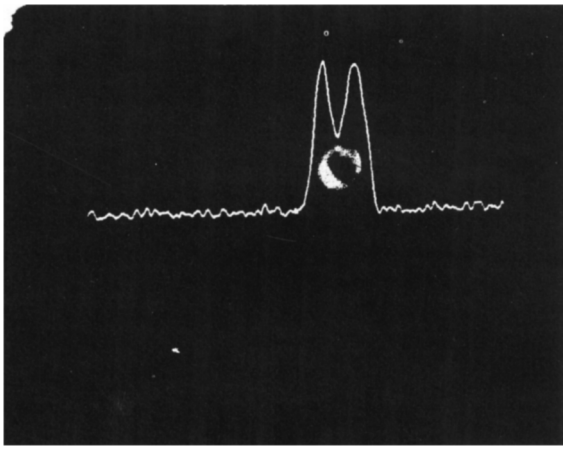

Figure 6 Partially sulfonated SDVB resin swollen with water. TR = 1 s.

regions will swell with solvent, whereas the unsulfonated organic region will not swell due to the hydrophobicity of the SDVB copolymer. This variation in solvent swelling should be easily visualized with MRI. Figures 5 and 6 show two images of an ion-exchange resin sulfonated only in an exterior circular region of the bead. The images show that solvent only swells the sulfonated regions of the resin. The interior, unsulfonated region shows no intensity—hence, no solvent swelling. This intensity distribution is also represented in the row profile shown in Figure 6. Changing the repetition time from 250 ms in Figure 5 to 1 s in Figure 6 does not affect the intensity in the image as it did in Figures 3 and 4. Therefore, the intensity is due to solvent that penetrates the sulfonated region and the lack of intensity represents the unswollen region that is hydrophobic. No saturation effects due to short repetition times relative to T_1 values are observed. This also eliminates partial sulfonation as one of the possible contributing factors for the inhomogeneity of solvent swelling observed in Figures 3 and 4. Since the intensity of the partially sulfonated bead is not affected by variation of TR, partial sulfonation is not a cause of the variation in solvent uptake observed in the beads of Figures 3 and 4 which do show intensity distribution differences dependent on the repetition time.

Ion-exchange resins are small so that the images of these beads could be improved using a smaller coil which would give a better filling factor. Figure 7 is an image of the same bead as Figure 4 taken using the Magnifier. The Magnifier, developed by Dave Cory at Bruker Instruments, is an insert placed in the imaging probe that has a coil with an i.d. of 2.5 mm. This small coil allows for an increase in the filling factor for small samples. Therefore, an increase in S/N of the image can be obtained or an image of comparable S/N can be obtained in less time. Figure 7 shows the bead to have the same intensity distribution as in Figure 4. The image in Figure 7 took only 1.2 h to acquire compared to 2.2 h for Figure 4 for comparable S/N. The profile shows the shoulder on the left representing the region of lower intensity due to less solvent swelling.

CONCLUSIONS

This study shows the first application of MRI to visualize solvent distribution in ion-exchange resins, sulfonated SDVB copolymers. Due to its noninvasive nature, MRI provides a map of the swollen

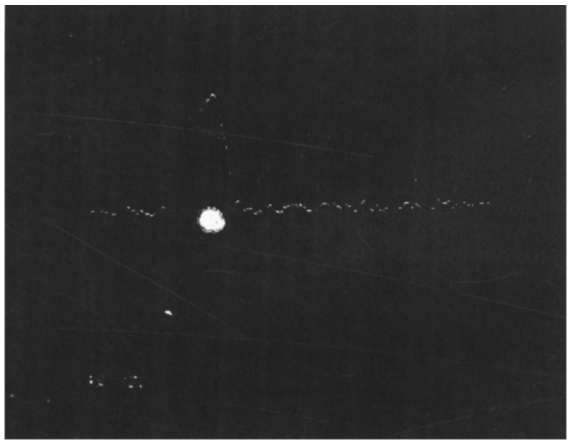

Figure 7 Sulfonated SDVB bead imaged with the Magnifier showing inhomogeneous swelling. Experiment time 1.2 h.

polymer network without interferences from staining dyes, stresses, and deformation due to cutting and addition of gold to aid in visualization in SEM. Images of beads that exhibit both homogeneous and heterogeneous swelling were examined. Also, partially sulfonated beads were imaged.

Images of multiple vs. single beads show that single-bead images are least affected by susceptibility differences and partial volume effects. Various single-bead mounting techniques showed that a capillary mounting method is the most efficient and suffers the least from susceptibility differences from nearby glass and physical deformations. Solvent does not evaporate from the bead during the time of data acquisition as was proven with repeated experiments of a bead with homogeneous solvent distribution. Resins which exhibit nonuniform swelling were imaged to differentiate the regions with differing solvent concentration. The solvent in these regions showed variations in T_1 values due to the amount of bulk and bound water in the particular region. Partially sulfonated SDVB resins showed that only the sulfonated regions were swollen and only those swollen regions have intensity in the image. The intensity distribution was not affected by T_1 weighting. A small coil, called the Magnifier, was used to increase the filling factor for small samples and allowed for an increase in S/N or a decrease in experiment time of nearly one-half in the given example for comparable S/N when compared to conventional 10 mm insert images.

REFERENCES

1. C. T. Kenner, *Analytical Determinations and Separations: A Textbook in Quantitative Analysis,* MacMillan, New York, 1971.
2. M. Okubo, M. Ando, A. Yamada, Y. Katsuta, and T. Matsumoto, *J. Polym. Sci. Polym. Lett.,* **19,** 143 (1981).
3. S. Lee and A. Rudin, *Makromol. Chem. Rapid Commun.,* **10,** 655 (1989).
4. I. Cho and K. W. Lee, *J. Appl. Polym. Sci.,* **30,** 1903 (1985).
5. M. Okuba, Y. Katsuta, and T. Matsumoto, *J. Polym. Sci. Polym. Lett.,* **18,** 481 (1980).
6. J. W. Vanderhoff, J. M. Park, and M. S. El-Aasser, *Proceed. ACS Div. Polym. Mater. Sci. Eng.,* **64,** 345 (1991).
7. S. Lee and A. Rudin, *Proceed. ACS Div. Polym. Mater. Sci. Eng.,* **64,** 281 (1991).
8. V. Dimonie, M. S. El-Aasser, and J. W. Vanderhoff, *Polym. Mater. Sci. Eng.,* **58,** 821 (1988).
9. S. R. Turner, R. A. Weiss, and R. D. Lundberg, *J. Polym. Sci. Polym. Chem. Ed.,* **23,** 535 (1985).
10. D. J. Lee and T. Ishikawa, *J. Polym. Sci. Polym. Chem. Ed.,* **21,** 147 (1983).
11. M. Okuba, Y. Katsuta, and T. Matsumoto, *J. Polym. Sci. Polym. Lett. Ed.,* **20,** 45 (1982).
12. M. Okuba, A. Yamada, and T. Matsumoto, *J. Polym. Sci. Polym. Chem. Ed.,* **16,** 3219 (1981).
13. J. Berg, D. Sundberg, and B. Kronberg, *Polym. Mater. Sci. Eng.,* **54,** 367 (1986).
14. D. J. Yarusso, S. L. Cooper, G. S. Knopp, and P. Georgopoulos, *J. Polym. Sci. Polym. Lett. Ed.,* **18,** 557 (1980).
15. Y. Okamoto, Y. Ueba, N. F. Dzhanibekov, and E. Banks, *Macromolecules,* **14,** 17 (1981).
16. J. S. Trent, J. I. Scheinbein, and P. R. Couchman, *J. Polym. Sci. Polym. Lett. Ed.,* **19,** 315 (1981).
17. J. S. Trent, J. I. Scheinbein, and P. R. Couchman, *Macromolecules,* **16,** 589 (1983).
18. A. S. Wallner, P. B. Smith, and W. M. Ritchey. Presented at the 34th ENC, Asilomar, CA, April 1992, paper 171.
19. P. B. Smith, The Dow Chemical Co., personal communication, 1992.
20. R. D. Kapadia, PhD Thesis, Case Western Reserve University, 1991.
21. E. Kokufuta and K. Saito, *J. Appl. Polym. Sci.,* **34,** 517 (1987).
22. S. Posse and W. P. Aue, *J. Magn. Reson.,* **88,** 473 (1990).
23. L. F. Czervionke, D. L. Daniels, F. W. Wehrli, L. P. Mark, L. E. Hendrix, J. A. Strandt, A. L. Williams, and V. M. Haughton, *A.J.N.R.,* **9,** 1149 (1988).
24. P. B. Smith, The Dow Chemical Co., personal communication, 1991.

Received March 25, 1994
Accepted October 6, 1994